Colitis ImmunoPET: Defining Target Cell Populations and Optimizing Pharmacokinetics

Jason L. J. Dearling, PhD,[*,†] Ala Daka, MS,[‡,§] Nuphar Veiga, BS,[‡,§] Dan Peer, PhD,[‡,§] and Alan B. Packard, PhD*[*,†]*

Background: Positron emission tomography combined with a specific probe presents the ability to noninvasively assess inflammatory bowel disease. We previously reported increased intestinal uptake of a ^{64}Cu-labeled anti-β_7 integrin antibody (clone FIB504.64) in colitic mice. Here, we evaluated an anti-$\alpha_4\beta_7$ integrin antibody (clone DATK32), and the F(ab′)$_2$ and Fab fragments of the anti-β_7 antibody, which should have faster blood clearance than the intact antibody, as imaging probes for the detection of colitis in a mouse model.

Methods: The immunoproteins were labeled with ^{64}Cu, injected into mice with dextran sodium sulphate-induced colitis. Positron emission tomography data were collected between 1 and 48 hours postinjection.

Results: Focal uptake of the anti-β_7 fragments was observed in the gut as early as 1 hour postinjection, and they cleared more rapidly from normal tissues than the whole antibody. For example, the blood concentrations at 24 hours postinjection were 23.3 ± 3.0% ID/g for ^{64}Cu-labeled DATK32, 12.9 ± 2.1% ID/g for FIB504.64, 4.1 ± 0.4% ID/g for FIB504.64-F(ab′)$_2$, and 0.62 ± 0.2% ID/g for FIB504.64-Fab ($P < 0.0001$, analysis of variance). The ratio of uptake of DATK32 between the colitis and control groups in the large intestine (1.38) was lower than for the FIB504.64 fragments (3.15 for F(ab′)$_2$, 1.84 for Fab) or intact FIB504.64 (1.78).

Conclusions: The lower intestinal uptake ratio of the ^{64}Cu-labeled anti-$\alpha_4\beta_7$ antibody (DATK32) compared with the anti-β_7 immunoproteins suggests that targeting all β_7-expressing lymphocytes, not just those expressing $\alpha_4\beta_7$, is a more promising route to the development of an inflammatory bowel disease imaging agent. The FIB504.64-F(ab′)$_2$ fragment demonstrated the greatest differential between colitis and control groups, and is therefore the most promising lead molecule for the development of an inflammatory bowel disease-specific imaging agent.

(Inflamm Bowel Dis 2016;22:529–538)

Key Words: inflammation imaging, β_7 integrin, FIB504.64, DATK32, copper-64

Inflammatory bowel disease (IBD), including ulcerative colitis and Crohn's disease, is a chronic autoimmune condition caused by the aberrant behavior of lymphocytes that affects approximately 1% of the population in Europe and North America.[1] Therapies include anti-inflammatory and immunosuppresive drugs with surgery appropriate in most cases. Assessment of the extent and degree of disease in the large intestine is usually made by colonoscopy, which is nonquantitative, operator-dependent, and invasive,[2] whereas disease of the small intestine requires entero–magnetic resonance imaging or entero–computed tomography.

Currently, no radiopharmaceutical is available specifically for positron emission tomography (PET) imaging of IBD. It is our overall aim to develop a colitis-specific PET imaging agent to provide real-time, quantitative, global information on the degree of disease, aiding in the diagnosis and therapy monitoring of individual patients.

One possible approach to the development of an IBD-specific imaging agent is to target the molecules involved in the recruitment and retention of the lymphocytes that are recruited and retained in the inflamed intestine. In IBD, lymphocytes are activated to express the integrin monomer β_7 by inductive sites such as Peyer's patches and mesenteric lymph nodes.[3] The β_7 monomer pairs with either an α_4 subunit to form $\alpha_4\beta_7$, which binds to the mucosal addressin cell adhesion molecule-1 for lymphocyte recruitment, or the α_E subunit to form $\alpha_E\beta_7$, which binds to E-cadherin for lymphocyte retention.[4] The aberrant behavior of the lymphocytes expressing these integrins results in the inflammation characteristic of IBD. Targeting the β_7 integrin may, therefore, lead to an IBD-specific imaging agent. Such an agent will present an advantage over other approaches in that it should allow discrimination between active colitis and the quiescent population of lymphocytes that populate the intestine.

Received for publication September 10, 2015; Accepted October 12, 2015.

From the *Division of Nuclear Medicine and Molecular Imaging, Department of Radiology, Boston Children's Hospital, Boston, MA; †Harvard Medical School, Boston, MA; ‡Laboratory of NanoMedicine, Department of Cell Research and Immunology, George S. Wise Faculty of Life Sciences, Department of Materials Science and Engineering, Faculty of Engineering; and §the Center for Nanoscience and Nanotechnology, Tel Aviv University, Tel Aviv, Israel.

Supported by National Institutes of Health Grant RC1 DK087348 (J.L.J.D., D.P., and A.B.P.), and the Children's Hospital Radiology Foundation (J.L.J.D. and A.B.P.). Supported in part by The Kenneth Ranin Foundation, FTA: Nanomedicine for Personalized Theranostics, and the The Leona M. and Harry B. Helmsley Nanotechnology Research Fund (D.P.).

The authors have no conflict of interest to disclose.

Reprints: Jason L. J. Dearling, PhD, Division of Nuclear Medicine and Molecular Imaging, Department of Radiology, Boston Children's Hospital, 300 Longwood Avenue, Boston, MA 02115 (e-mail: jason.dearling@childrens.harvard.edu).

DOI 10.1097/MIB.0000000000000677

Published online 3 February 2016.

We previously reported increased uptake of the ^{64}Cu-labeled anti-β_7 antibody FIB504.64 in the large intestines of mice with colitis compared with controls.[5] This was a very encouraging initial result, but it suggested several possible refinements including the possibility of better defining the target cell population and increasing the clearance rate of the imaging agent from the blood to decrease the time between injection of the agent and image acquisition. With respect to better defining the target cell population, the antibody DATK32 binds to the $\alpha_4\beta_7$ integrin, which is expressed by the subset of lymphocytes that are involved in recruitment.[6] With respect to improving the clearance rate, whereas the clearance rate of intact mAbs (molecular weight 150 kDa) is typically on the order of several days, the clearance rate of the F(ab′)$_2$ (110 kDa) and Fab (50 kDa) antibody fragments is much shorter, typically only a few hours, which can significantly decrease the time required for the tracer to achieve acceptable target-to-background ratios. The drawback to using antibody fragments is that the absolute uptake at the target site is decreased.[7]

In this study, we investigated both of these approaches to the development of an IBD-specific imaging agent. First, we compared the ^{64}Cu-labeled anti-$\alpha_4\beta_7$ antibody DATK32, which is specific for $\alpha_4\beta_7$ integrin-expressing leukocytes, to the ^{64}Cu-labeled anti-β_7 antibody FIB504.64, which binds to both $\alpha_4\beta_7$ and $\alpha_E\beta_7$ expressing leukocytes. Second, we compared the biodistribution of the ^{64}Cu-labeled F(ab′)$_2$ and Fab FIB504.64 fragments to the biodistribution of the whole ^{64}Cu-labeled FIB504.64.

MATERIALS AND METHODS

General

Chemicals and reagents were obtained from Sigma–Aldrich (St. Louis, MO) unless otherwise specified. The zero-length linker 1-ethyl-3-(3-(dimethylamino)propyl) carbodiimide hydrochloride (EDC) was purchased from Pierce (Rockford, IL). The bifunctional chelators (BFCs) S-2-(4-aminobenzyl)-1,4,7,10-tetraazacyclododocane tetraacetic acid (p-NH$_2$-Bn-DOTA) and S-2-(4-isothiocyanatobenzyl)-1,4,7-triazacyclononane-1,4,7-triacetic acid (*p*-NCS-Bn-NOTA) were purchased from Macrocyclics (Dallas, TX). Metal-naive pipette tips were purchased from Rainin (Oakland, CA). Glass and plasticware were washed with 10% HNO_3 and rinsed thoroughly with ultrapure water (>15 MΩ resistivity; Siemens, Lowell, MA) before use. Ultrapure water was also used in buffer preparation. Sodium acetate buffer (0.1 M, pH 5.0) was used for conjugation (EDC reaction) and radiolabeling. Metal contaminants in the buffer were decreased by passing it through a Chelex-100 resin column (Bio-Rad Laboratories, Hercules, CA). Copper-64 was produced at the Washington University School of Medicine (St. Louis, MO). Radioactivity was assayed using a Packard Cobra II automated gamma counter (Meriden, CT). Small animal PET data were obtained using a Siemens Focus 120 camera (Siemens Medical Solutions USA, Malvern, PA).

Experimental Colitis Model

Dextran sodium sulphate (DSS; 36–50 kDa, MP Biomedicals, Solon, OH), which is known to induce inflammation throughout the bowel principally affecting the large intestine,[8–10] was included in the drinking water at 2.0% (wt/vol). Under this regimen, colitis typically develops after approximately 9 days. Tissue and cellular effects of DSS treatment were studied using mouse endoscopy and fluorescent immunohistochemistry.

Mouse Endoscopy

After 9 days of DSS treatment, the severity of colitis was assessed by colonoscopy as previously described.[11] Mice (n = 6 in each group) were anesthetized using ketamine-xylazine (80 mg/kg ketamine and 15 mg/kg xylazine). A mouse endoscope was used to view the severity of colitis, which was scored according to the murine endoscopic index of colitis severity scoring system, which includes 5 parameters — feces consistency, vascularity, transparency, granularity, and fibrin presence.[11] Each parameter was scored from 0 to 3, with a total score of 0 to 4 considered healthy and 8 to 11 indicating disease.

Fluorescent Immunohistochemistry

Colon tissue from control and DSS-treated mice was frozen in isopentane, cooled in a slurry of isopropane and solid carbon dioxide, and then stored at −80°C. Sections (10 μm) were taken using a cryotome and mounted on polylysine-coated slides, air dried, and then fixed in methanol. The sections were rehydrated with phosphate-buffered saline (0.1 M, pH 7.4), blocked with donkey serum, probed with anti-β_7 FIB504.64 antibody (80 μg/mL) or anti-$\alpha_4\beta_7$ DATK32 antibody (92.4 μg/mL), and incubated for 1 hour. The sections were washed and the secondary antibody (donkey anti-rat) conjugated with Alexafluor A647 (Life Technologies, Grand Island, NY) was applied (5 μg/mL). The primary antibody was not applied to the control sections. After one hour, the sections were washed and mounted using Prolong Gold antifade mounting media (Life Technologies, Grand Island, NY) for observation.

Antibody Production

The anti-β_7 antibody FIB504.64 and the anti-$\alpha_4\beta_7$ antibody DATK32 were produced from their hybridomas and purified using a HiTrap Protein G column (GE Healthcare, Piscataway, NJ). Antibody fragments F(ab′)$_2$ and Fab (Fig. 1) were produced using standard molecular biology techniques, purified, and confirmed using Western blot analysis.

Antibody-chelator Conjugation

DATK32 Conjugation with p-NH$_2$-Bn-DOTA

The antibody was buffer exchanged into sodium acetate (0.1 M, pH 5.0) and concentrated to approximately 10 mg/mL using spin column filters (Centricon; Millipore, Bedford, MA; MWCO 30 kDa). The BFC *p*-NH$_2$-Bn-DOTA was conjugated to the antibody using established methods. Briefly, to *p*-NH$_2$-Bn-DOTA in Me$_2$SO (100 mg/mL) was added 3 volume equivalents of

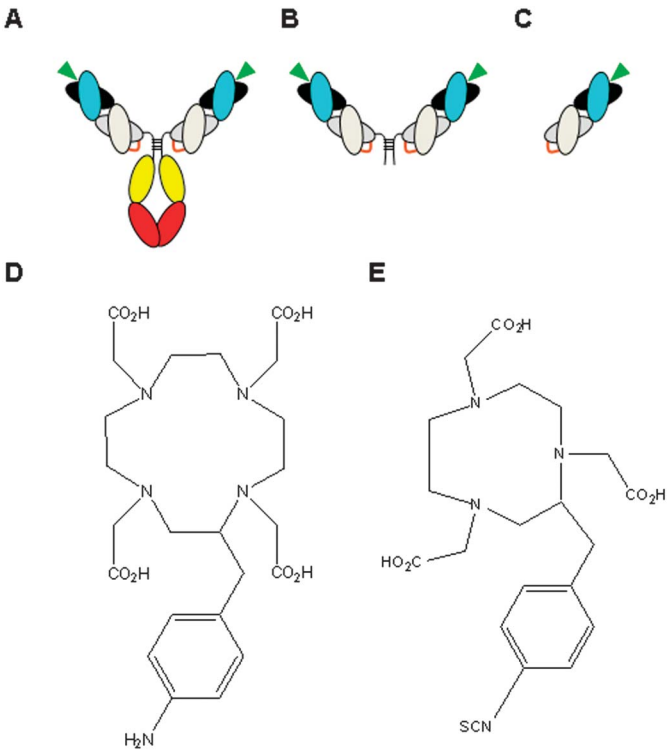

FIGURE 1. Structures of the proteins and bifunctional chelators used in this study. Top row: Whole antibody (A), F(ab')$_2$ (B), and Fab (C). Bottom row: *p*-NH$_2$-Bn-DOTA (D) and *p*-SCN-Bn-NOTA (E).

0.1 M sodium acetate buffer (pH 5.0) to give a final BFC concentration of 25 mg/mL, and the pH was brought to 5.0 by addition of 1 N NaOH. The chelator was added to the antibody at a molar ratio of 250:1, and then 500 molar equivalents of EDC, which was made up immediately before use in ultrapure water at a concentration of 50 mg/mL, was added. The final antibody concentration after addition of all reagents was 5 mg/mL. The reaction was gently mixed by pipetting, centrifuged to remove air bubbles, the pH was confirmed to be 5.0, and then the reaction mixture was placed in a 37°C water bath. The final concentration of Me_2SO was always <5% (typically <1%). After 30 minutes at 37°C, the reaction was removed from the water bath and unbound chelator was separated from the immunoconjugate by size exclusion high performance liquid chromatography (HPLC) (BioSep SECS3000 column; Phenomenex, Torrance, CA) with an aqueous phase of 0.1 M sodium acetate, pH 5.0. The retention time of the immunoconjugate was typically 8.1 minutes, with the unbound chelator eluting at approximately 11.0 minutes. The purified immunoconjugate fractions were pooled, concentrated using spin column filters (30 kDa MWCO), and stored in aliquots at −80°C.

FIB504.64-F(ab')$_2$ and FIB504.64-Fab Conjugation with p-NCS-Bn-NOTA

The conjugation of *p*-NCS-Bn-NOTA to the FIB504.64 fragments was performed as described by Vosjan et al.[12] Briefly, the protein was buffer exchanged into sodium carbonate buffer (0.1 M, pH 9.0), and the BFC was added at a molar ratio of 3:1 in 3 aliquots separated by 5 minutes (i.e., final molar ratio of protein to BFC = 1:3). The reaction mixture was mixed by gentle pipetting after each addition and then placed in a water bath at 37°C for 1 hour. Unbound chelator was removed by HPLC as before, the immunoconjugate was concentrated using spin column filters (30 kDa MWCO) and stored in aliquots at −80°C.

DOTA was used as the BFC to label DATK32 with ^{64}Cu, despite its well-known limitations,[13] so that the results of this study could be directly compared with those from our previous study with ^{64}Cu-DOTA-FIB504.64.[5] NOTA was used as the BFC for labeling the antibody fragments because it has recently emerged as a more kinetically stable BFC for labeling proteins with ^{64}Cu.

Immunoreactivity Assay

The immunoreactivity of the BFC-conjugated antibody was assayed by flow cytometry.[14] Briefly, 10^6 TK-1 cells (mouse T cells lymphoma) expressing $\alpha_4\beta_7$ integrin were stained with 10 μg/mL purified antibody or with its corresponding immunoconjugate for 30 minutes at 4°C. The cells were then washed twice with FACS buffer (phosphate-buffered saline including 2% fetal calf serum) and counterstained with a second, Alexa-488-labeled,

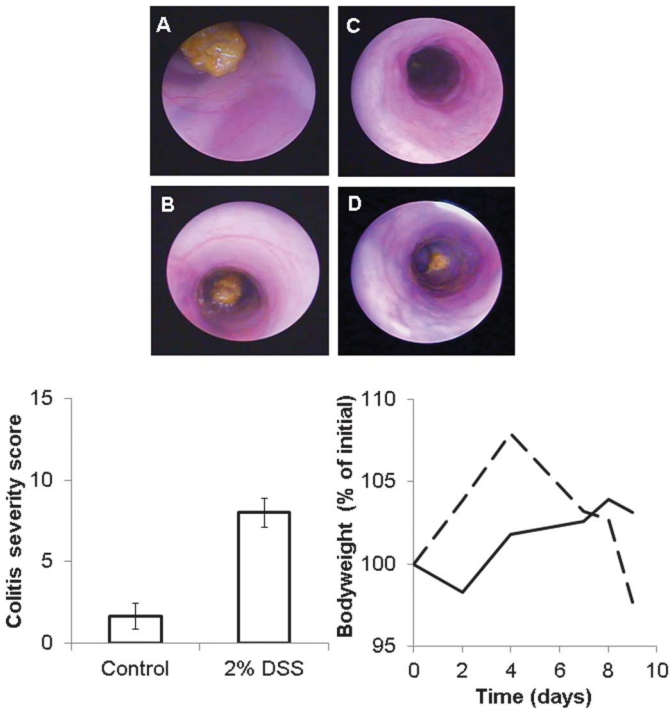

FIGURE 2. Evaluation of DSS-induced colitis model. Example images of the colons of control mice (A and B) and those of mice in the DSS-treated group (C and D) are shown. These were scored according to the murine endoscopic index of colitis severity scale, and the scores for the 2 groups (bar graph) were significantly different ($P < 0.001$). The effect of the model on body weight (line graph) is shown in the line graph comparing control (solid line) and DSS-treated groups (dashed line).

mAb against rat IgG2a at 4°C for 30 minutes and subjected to flow cytometry (FACScan; BD Biosciences, San Jose, CA).

Radiolabeling

For imaging studies, the immunoconjugates were radiolabeled with ^{64}Cu as previously described.[5] For example, to 2 mCi ^{64}Cu in 5 to 10 μL HCl (0.04 N) was added 3 volume equivalents of acetate buffer (pH 5, 0.1 M). To this was added the antibody (e.g., 250 μg, 75 μL), also in acetate buffer. After 30 minutes of incubation at 25°C, 1 μL of the reaction was added to 9 μL phosphate buffer (PB; 0.1 M, pH 8) containing 100 mM ethylenediamine-tetraacetic acid (EDTA). After 5 minutes, 1 μL of the solution was spotted onto an ITLC plate (ITLC SG; Biodex, Shirley, NY), which was allowed to air-dry and then developed using PB/100 mM EDTA as the mobile phase. The plate was cut into 4 sections and radioactivity in the sections was assayed using a gamma counter. Using these conditions, labeled antibody remains at the baseline of the plate with free copper moving with the solvent front. If the radiochemical purity was less than 95%, the labeled Ab was purified using Centricon spin filters. Once the radiochemical purity of the labeled Ab was 95% or greater, it was diluted to a protein concentration of 500 μg/mL and sterile filtered (0.2 μm) before injection.

Biodistribution Studies

After colitis was established in the mice, the ^{64}Cu-labeled antibody was injected into the tail vein (50 μg protein, 2.0–6.8 MBq [54–183 μCi], in 0.1 mL saline). Small animal PET data were collected for 30 minutes at 1, 24, and 48 hours postinjection (p.i.) for the DATK32 studies, and at 1, 4, and 24 hours p.i. for the FIB504.64-F(ab′)$_2$ and FIB504.64-Fab studies. Different data collection schedules were used because of the large differences in clearance half-lives between the whole antibodies and the much smaller fragments. After the final imaging study, the mice were killed by CO_2 inhalation and an ex vivo biodistribution study was performed. Selected tissues were collected, weighed, and radioactivity was measured. Small animal PET images were analyzed using AMIDE software.[15] Data from volumes of interest (VOIs) within tissues of interest (liver, kidney, lung, muscle, brain, and gut) were used to calculate biodistribution throughout the imaging study.

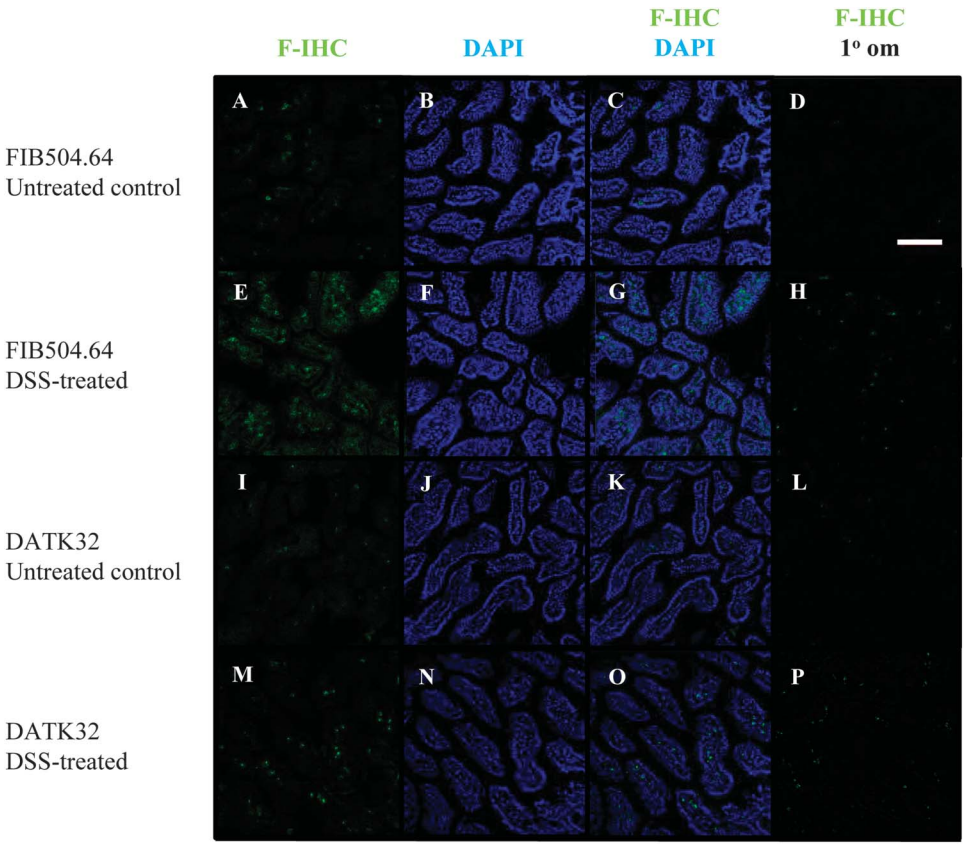

FIGURE 3. Images of frozen sections of mouse colon stained for imflammation targets using fluorescent immunohistochemistry. These images show the larger population of target β_7 integrin monomer positive cells and $\alpha_4\beta_7$ positive cells in DSS-treated colon compared with controls. Control or DSS-treated tissue was stained for β_7 integrin monomer using antibody FIB504.64 (A–H), or $\alpha_4\beta_7$ integrin using antibody DATK32 (I–P). Antibody binding was detected using a donkey anti-rat IgG2a secondary antibody. The tissue was counter-stained with DAPI to show cell nuclei (B–N), and these 2 images were overlaid for comparison (C–O). Panels D–P show the low level of staining obtained when the primary antibody was omitted. Scale bar is 100 μm (D).

Statistical Analysis

Statistical analyses were performed using GraphPad Prism (Version 5.04) for Windows (GraphPad Software, La Jolla, CA). Ex vivo biodistribution data for control and DSS treated groups were compared using a 2-tailed, unpaired Student's *t* test. Differences were considered statistically significant at the 5% level ($P < 0.05$). Unless otherwise stated, data are reported as the mean (±SD).

ETHICAL CONSIDERATIONS

All animal procedures were performed under a protocol approved by the Boston Children's Hospital Institutional Animal Care and Use Committee or the Tel-Aviv University Institutional Animal Care and Use Committee.

RESULTS

Experimental Colitis Model

Example images of inflamed colon and the murine endoscopic index of colitis severity inflammation scores are presented in Figure 2. The score for control mice (1.7 ± 0.8) was significantly different from that for DSS-treated mice (8.0 ± 0.9, $P < 0.001$). Colitis caused by DSS resulted in the characteristic increase and then decrease in body weight (Fig. 2) as reported previously.[5]

The cellular effects of DSS treatment were investigated using fluorescent immunohistochemistry. Images of the distribution of β_7- and $\alpha_4\beta_7$-positive cells are shown in Figure 3. There are fewer β_7-positive cells in control mouse colon (3A) than in the abluminal regions of the DSS-treated colon (3E). Similarly, there are fewer $\alpha_4\beta_7$-positive cells in untreated mouse colon (3I) than in DSS-treated colon (3M). The population of $\alpha_4\beta_7$-positive cells in DSS-treated colon (3M) is smaller than the total β_7-positive population (3E).

Comparing the blood clearance of the proteins, for the 2 intact antibodies the radioactivity in the blood for DATK32, the anti-α4β7 antibody, at 24 hours p.i. was 23.3 ± 3.0% ID/g compared with 12.9 ± 2.1% ID/g for FIB504.64, the whole anti-β7 antibody (Fig. 4).[5] As anticipated, at 24 hours p.i. the concentration of the antibody fragments in the blood was much lower than that of the intact antibodies (FIB504.64-F(ab′)$_2$: 4.09 ± 0.4% ID/g; FIB504.64-Fab: 0.62 ± 0.2% ID/g).

Antibody Radiolabeling

The BFC-conjugated antibodies retained antigen binding as evidenced by flow cytometry (data not shown). They were radiolabeled with ^{64}Cu to specific activities of 74 to 146 MBq/mg (2–4 mCi/mg). Radiochemical purity was always >95% before injection.

In vivo Distribution of Anti-$\alpha_4\beta_7$ and Anti-β_7 Immunoproteins

Small animal PET data were collected from 1 to 48 hours p.i. (Fig. 5). Values from organ VOIs were converted to %ID/g and are presented as bar graphs in Figure 6. For the anti-$\alpha_4\beta_7$ whole antibody, uptake in the gut region was lower than for anti-β_7 whole antibody, but higher than for the smaller molecules. Uptake of DATK32 in the large intestine was 3.8 ± 0.5% ID/g (4.6 ± 0.5% ID/g in the control group), whereas intestinal uptake of FIB504.64 was 5.7 ± 2.0% ID/g (4.4 ± 1.2% ID/g in healthy controls). Overall, its tissue distribution is typical for a whole antibody, with higher uptake in liver, kidney, and lung, reflecting antibody excretion pathways and tissues containing large amounts of blood.

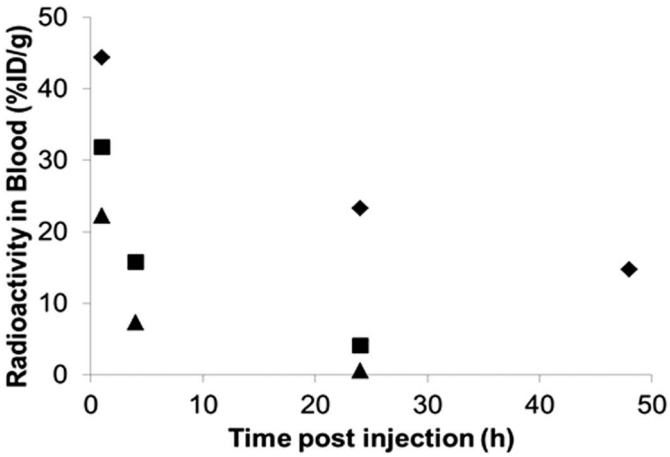

FIGURE 4. Blood pharmacokinetics of the radiolabeled antibodies in mice. The whole anti-$\alpha_4\beta_7$ antibody (DATK32, diamonds) cleared less rapidly than the anti-β_7 antibody fragments FIB504.64-F(ab′)$_2$ (squares) and FIB504.64-Fab (triangles).

Uptake of FIB504.64-F(ab′)$_2$ in the gut of DSS-treated mice was higher than in the controls at 4 hours p.i. (DSS-treated, 7.7 ± 2.0% ID/g; controls, 4.8 ± 0.4% ID/g, $P = 0.053$) and had cleared by 24 hours for the control group (2.2 ± 0.5% ID/g) but remained stable for the DSS-treated mice (4.8 ± 2.3% ID/g). The tissue with the highest uptake was the kidney, which reached a peak at 4 hours (DSS-treated, 37.7 ± 7.8% ID/g; controls, 33.4 ± 6.5% ID/g). Uptake in the liver was very low for a ^{64}Cu-labeled protein (DSS-treated, 10.1 ± 2.0% ID/g; controls, 6.4 ± 1.4% ID/g), particularly in comparison with the intact DATK32 Ab, which was labeled with ^{64}Cu using DOTA rather than NOTA as the BFC (^{64}Cu-DOTA-DATK32 liver uptake was 11.2 ± 1.2% ID/g in the control group and 10.1 ± 1.4% ID/g in the DSS-treated group).

Gut uptake of the FIB504.64-Fab molecule was higher in the colitis group than the control group at 4 hours (DSS-treated, 5.9 ± 0.9% ID/g; controls, 3.3 ± 1.5% ID/g; P = 0.017), and then cleared rapidly by 24 hours p.i. (DSS-treated, 2.2 ± 1.1% ID/g; controls, 1.4 ± 0.3% ID/g). Kidney uptake was high at 4 hours p.i. (DSS-treated, 34.6 ± 11.3% ID/g; controls, 22.4 ± 10.2% ID/g) and decreased by the 24 hours time point (DSS-treated, 17.2 ± 4.5% ID/g; controls, 9.1 ± 1.3% ID/g).

The gut uptake concentration data are the mean of a VOI drawn in the abdomen of the mice, which includes both the uptake

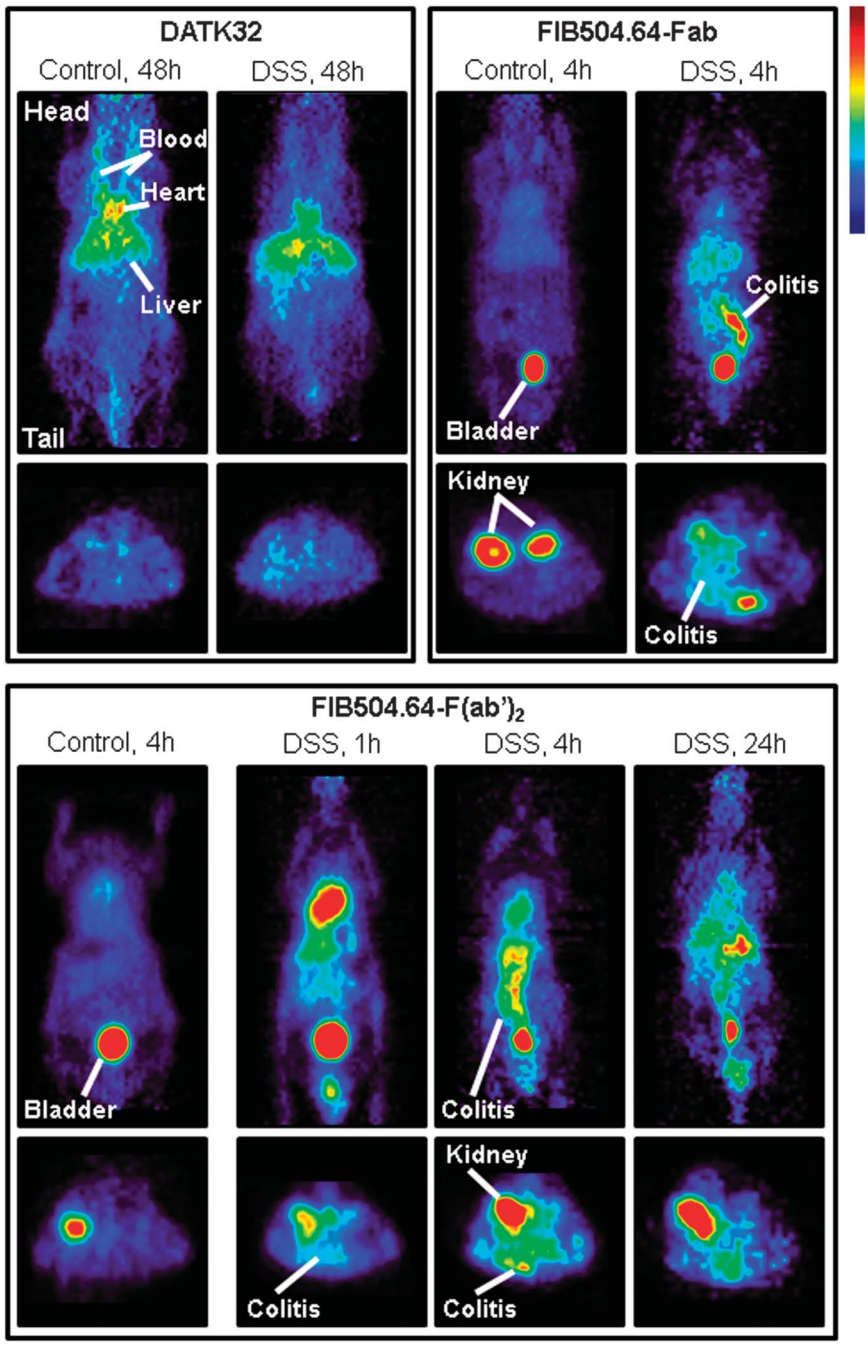

FIGURE 5. Small animal PET images. Example coronal (top) and transaxial (bottom) images are presented showing the distributions of the radiolabeled proteins (scale bar top right). The distribution of the DATK32 antibody was typical for an antibody, with radionuclide in the blood and liver, and slightly higher uptake in the gut of DSS-treated mice at 48 hours p.i. Uptake of the FIB504.64-Fab in the gut was highest at 4 hours p.i. Gut uptake of the FIB504.64-F(ab')$_2$ was evident at 1 hour, high at 4 hours (control at 4 h presented for comparison), and persisted out to 24 hours p.i.

in the gut itself and background. These data do not, therefore, adequately represent the foci of high uptake evident in the images of the DSS-treated mice. To better represent these foci of activity in the gut VOIs, the %ID/g for each voxel was calculated for one mouse from each of the six groups (DATK32, Fab and F(ab')$_2$; treated and control) at each imaging time point. These data are presented in Figure 7 as count-frequency graphs where the %ID/g in each voxel is plotted against the frequency with which each %ID/g value occurs. Thus, background uptake is represented by a large number of voxels with low %ID/g to the left of the graph, whereas focal uptake results in peaks to the right of the graph with higher %ID/g values.

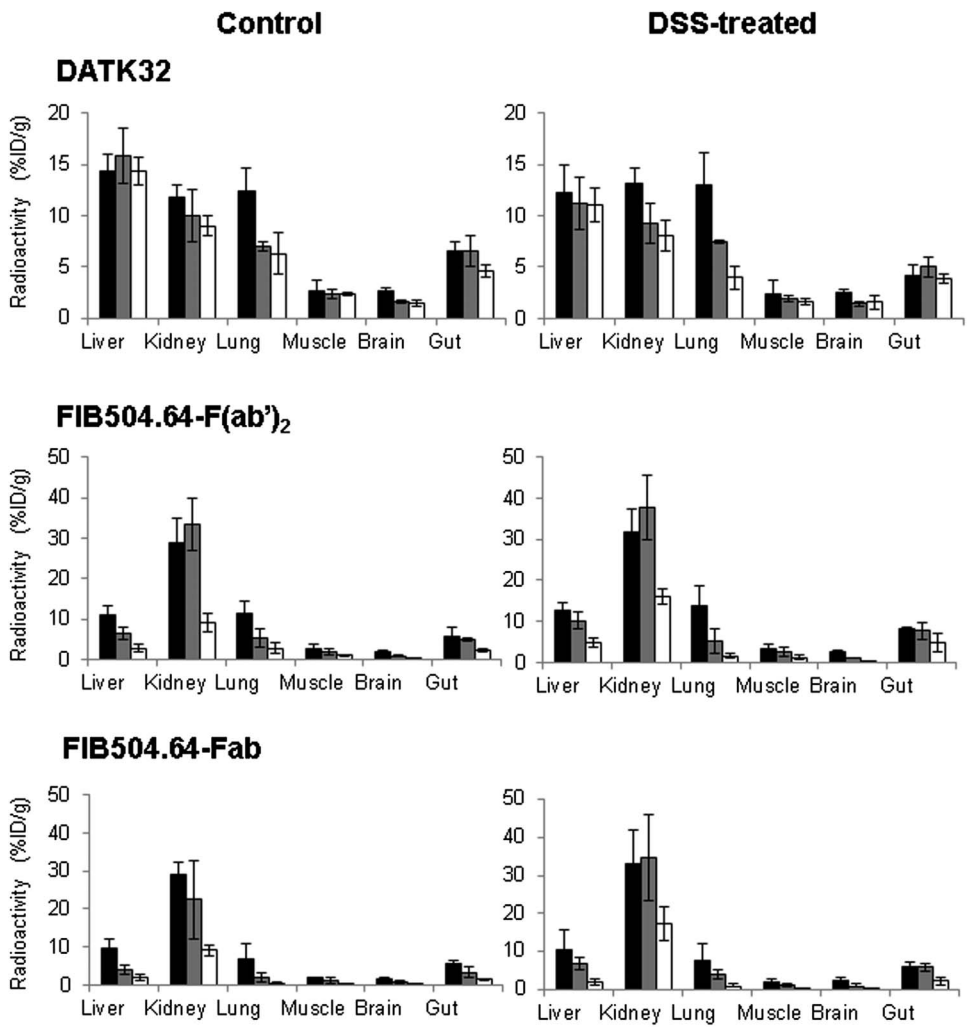

FIGURE 6. Bar graphs of imaging-based biodistribution of gut uptake of the radiolabeled antibodies at 1, 4 and 24 hours post injection (black, gray, and white bars, respectively). The distribution of the whole antibody DATK32 was typical for a whole antibody, with slow clearance from normal tissues (mean %ID/g, error bars SD). In contrast, the radiolabeled antibody fragments show higher uptake in the kidney compared with the whole antibodies. Note differences in y-axes.

The data for the anti-$\alpha_4\beta_7$ antibody DSS-treated group are consistent throughout the study, with all 3 data sets approximating a symmetric distribution centered on 2% ID/g. In contrast, whereas the control group data starts with a large peak at approximately 2% ID/g at 1 hour p.i., the maximum value shifts to 6% ID/g at 24 hours p.i. and then decreases to 4% ID/g at 48 hours p.i.

The count frequency graphs for the anti-β_7 antibody fragments FIB504.64-F(ab′)$_2$ and FIB504.64-Fab look quite different from those observed for the anti-$\alpha_4\beta_7$ whole antibody. For the DSS-treated animals, the data for antibody fragments reveal a more heterogeneous distribution with a large number of voxels with high uptake values at 1 and 4 hours with a peak at 12% to 14% ID/g for FIB504.64-F(ab′)$_2$ and a peak at approximately 5% ID/g for FIB504.64-Fab. For FIB504.64-F(ab′)$_2$, the 24 hour p.i. data resolves toward a more normal distribution centered at approximately 7% ID/g, 3 to 4 times higher than in the control animals. For FIB504.64-Fab, the 24 hour data are very similar to that for the control animals suggesting for rapid clearance for FIB504.64-Fab than for divalent (and slower clearing) FIB504.64-F(ab′)$_2$.

Ex vivo Distribution of Anti-$\alpha_4\beta_7$ and Anti-β_7 Immunoproteins

Biodistribution data for the 3 proteins in the control and DSS-treated mice and the results from statistical analysis of these data are shown in Table 1.

For all 3 proteins, uptake in the stomach, small intestine, and large intestine tended to be higher in the mice with colitis than in the control group. This difference is statistically significant ($P < 0.05$) for the anti-$\alpha_4\beta_7$ antibody in large intestine (3.61 versus 2.61% ID/g), as it is for the anti-β_7 antibody (6.49 versus 3.64% ID/g) and for its fragment FIB504.64-F(ab′)$_2$ in stomach (1.67 versus 0.95% ID/g) and large intestine (5.46 versus 1.74%

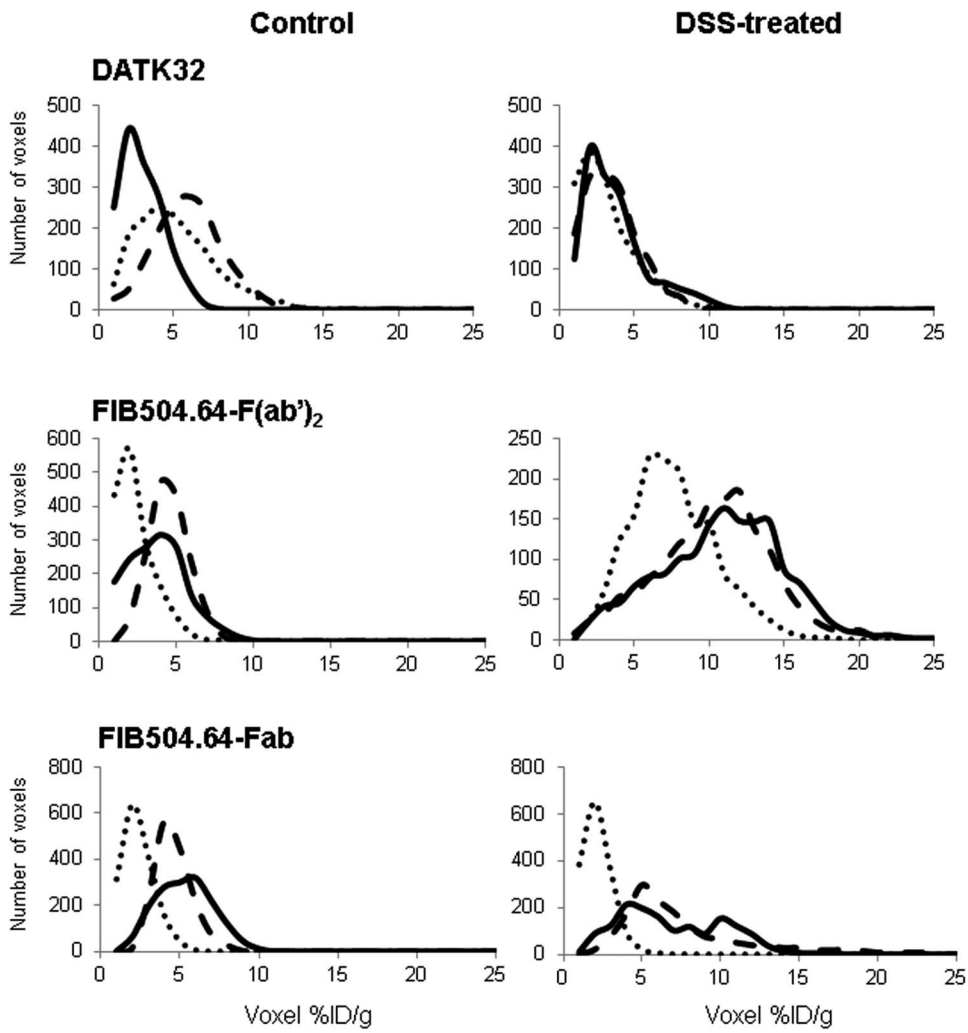

FIGURE 7. Count-frequency line graphs of gut uptake of the radiolabeled antibodies reflecting the heterogeneity of radiolabeled antibody distribution at 1, 4 and 24 hours post injection (solid, dashed, and dotted line, respectively). The data for the control animal approximates a normal distribution whereas that for the test animal represents the focal high uptake in regions of inflammation. Note differences in y-axes.

ID/g), but the differences were not statistically significant for FIB504.64-Fab. The observation that larger differences between DSS-treated and control animals are observed in the large intestine than in other regions of the gut is consistent with the fact that DSS is known to have a greater effect on the large intestine than on the rest of the digestive tract.[8] The distribution of the ^{64}Cu-labeled anti-$\alpha_4\beta_7$ antibody in nontarget tissue is typical for an antibody with some uptake in the liver and spleen and low uptake in muscle, bone, and brain. Kidney uptake of the smaller fragments was higher in the DSS-treated mice than in control animals (FIB504.64-F(ab′)$_2$: DSS-treated, 28.1% ID/g; control, 13.7% ID/g; FIB504.64-Fab: DSS-treated, 37.4% ID/g; control, 17.2% ID/g).

DISCUSSION

We previously reported increased accumulation of the ^{64}Cu-labeled anti-β7 antibody FIB504.64 in the intestine of DSS-treated mice.[5] In this study, we extended this investigation using the ^{64}Cu-labeled anti-$\alpha_4\beta_7$ antibody DATK32, which only targets $\alpha_4\beta_7$-positive lymphocytes, the subset of the total leukocyte population that is involved in the recruitment of lymphocytes to sites of inflammation. We assessed the populations of β_7- and $\alpha_4\beta_7$-positive cells in the colons of DSS-treated mice using fluorescent immunohistochemistry and found that, as expected, the $\alpha_4\beta_7$ population was smaller. This provides a reasonable explanation for why the ratio of intestinal uptake in control and colitis groups is lower for DATK32 than for FIB504.64 (ratio of uptake in colitic and control large intestine: FIB504.64 = 1.78; DATK32 = 1.38). This result also suggests that there is no strong rationale for further development of DATK32 as a PET agent for colitis. We therefore turned to the goal of improving the pharmacokinetics of ^{64}Cu-labeled FIB504.64. Specifically, we reduced the size of the protein to increase its clearance rate from normal tissues, and decrease the time required between injection of the tracer

TABLE 1. Ex Vivo Biodistribution of the Radiolabeled Antibodies in Control and DSS-treated Mice at 48 Hours (DATK32) or 24 Hours (FIB Fragments) Post Injection

	DATK32		FIB504.64-F(ab′)$_2$		FIB504.64-Fab	
	Control	DSS	Control	DSS	Control	DSS
Blood	**14.8 (2.2)**	**9.41 (3.3)**	4.46 (1.8)	4.09 (0.4)	0.45 (0.2)	0.51 (0.1)
Heart	4.43 (1.3)	3.20 (0.8)	1.96 (0.6)	2.30 (0.6)	**0.57 (0.2)**	**1.15 (0.2)**
Lung	7.24 (1.2)	8.82 (4.3)	3.52 (0.3)	3.22 (0.3)	1.74 (1.4)	1.72 (0.2)
Liver	11.2 (1.2)	10.1 (1.4)	**2.54 (0.6)**	**4.35 (0.7)**	**1.9 (0.5)**	**3.07 (0.2)**
Spleen	8.95 (1.8)	11.5 (2.7)	7.73 (0.7)	9.46 (4.2)	4.92 (2.8)	5.21 (2.0)
Kidney	7.58 (0.9)	6.11 (1.6)	**13.7 (4.0)**	**28.1 (5.3)**	**17.2 (6.7)**	**37.4 (10.2)**
Brain	0.46 (0.07)	0.37 (0.1)	0.14 (0.05)	0.13 (0.04)	0.04 (0.02)	0.05 (0.0)
Muscle	1.00 (0.3)	0.93 (0.4)	**0.54 (0.1)**	**0.36 (0.04)**	0.16 (0.07)	0.26 (0.1)
Bone	2.43 (0.9)	2.15 (0.8)	1.45 (0.2)	1.35 (0.27)	0.63 (0.09)	1.27 (0.9)
Stomach	1.97 (0.5)	2.56 (1.9)	**0.95 (0.04)**	**1.67 (0.4)**	0.74 (0.6)	0.85 (0.1)
		1.30		*1.75*		*1.15*
Small intestine	3.14 (0.3)	3.32 (0.5)	2.23 (0.5)	3.61 (1.5)	1.44 (0.4)	1.80 (0.7)
		1.06		*1.61*		*1.25*
Large intestine	**2.61 (0.2)**	**3.61 (0.8)**	**1.74 (0.5)**	**5.46 (2.4)**	1.65 (0.6)	3.04 (1.7)
		1.38		*3.15*		*1.84*
N =	5	5	3	4	5	4

Data presented are means of % injected dose per gram (SD in parenthesis). Italic font indicates the ratios of control to DSS data, bold font indicates significant difference ($P < 0.05$) between control and DSS-treated groups (Student's *t* test).

and imaging whereas hoping to maintain a high target-to-background ratio. The caveat to this approach is that increasing the clearance rate also tends to decrease the absolute uptake of tracer in the target tissue. This approach has proved to be useful in tumor imaging[7]; but to the best of our knowledge, it has not yet been applied to imaging inflammation.

In these studies we found that, whereas the clearance of the Fab molecule from nontarget tissues was more rapid than for the F(ab′)$_2$, the ratios between control and colitic gut uptakes for the F(ab′)$_2$ were higher, primarily due to higher uptake in the inflamed tissue. Also, uptake of the tracer in the inflamed gut seems to be relatively more sustained for the F(ab′)$_2$ compared with the Fab, as indicated by the higher peak of the count-frequency graph data at 24 hours. These effects probably result from the divalent binding of the F(ab′)$_2$ fragment to the integrin target compared with the monovalent binding of the Fab fragment.

Although ^{64}Cu-labeled DATK32 did not have the highest uptake ratio between control and inflamed intestine of the 4 tracers that we examined in this study, the ratio was greater than 1 (1.38). It could, therefore, still prove useful in the evaluation of diseases that are caused by overexpression of the $\alpha_4\beta_7$ integrin. The $\alpha_4\beta_7$ integrin is also a viable therapeutic target, especially given that the $\alpha_4\beta_7$-positive lymphocyte population is predominantly responsible for cytokine production (Interferon-gamma and tumor necrosis factor-alpha) in IBD.[16] In this context, it is worth noting that the count frequency distribution of ^{64}Cu-labeled DATK32 in the colitis group did not show focal uptake at higher %ID/g values suggesting that this tracer (and thus the target) is relatively evenly distributed throughout the gut. In contrast, the intestinal uptake of ^{64}Cu-labeled FIB504.64 and its Fab and F(ab′)$_2$ fragments, which bind to the β_7 integrin monomer, is focal, suggesting that the hot spots may be due to relatively high local concentrations of $\alpha_E\beta_7$-positive lymphocytes.

One limitation of this study is the use of the DSS colitis model. Although the DSS model is useful because it is highly defined and predictable, resulting in colitis after 7 to 10 days, other models, such as the T-transfer and Tbet KO model[17,18] produce a colitis model with histopathological features that more closely replicate those in human disease.

Another consideration is the radiation exposure to patients during PET and computed tomography imaging. Typically, a PET procedure will result in an absorbed dose of approximately 7 mSv and a computed tomography scan will result in an absorbed dose of approximately 10 mSv. To put this exposure in context, the average annual radiation exposure from background sources in the United States is 3.11 mSv.[19]

One unexpected observation in this study was the higher uptake of the ^{64}Cu-labeled antibody fragments in the kidneys of the colitic mice. Although higher renal accumulation of the antibody fragments was expected because smaller proteins tend to excreted by the kidneys, the 2-fold higher renal uptake of both antibody fragments in colitic versus control animals was not expected. This increased uptake could be due to a number of factors related to the effects of DSS treatment such as dehydration, which would result in

slower clearance. There was also a 20% difference in kidney weight between the 2 groups (DSS-treated group 142 ± 38 mg, n = 13; control group 176 ± 40 mg, n = 12, $P < 0.05$). Interestingly, kidney uptake of the radiolabeled FIB504.64 and DATK32 antibodies in DSS-treated mice was slightly lower than in control mice.

Poor renal function is a common symptom in patients with colitis. Ranganathan et al[20,21] examined the role of chemokines in the interaction between the inflamed colon and the kidney and found significant biological effects, including increased serum creatinine levels (a marker of kidney damage), tubular injury, and plugging of blood vessels by red blood cells. These changes may have contributed to the differences observed in this study. Furthermore, changes in kidney function are relevant to the clinical translation of imaging agents such as these because increased tracer uptake by the kidneys will lead to a corresponding increase in the radiation dose to the kidneys.

In this study, we expanded on our previous study of PET imaging of colitis using ^{64}Cu-labeled FIB504.64 by investigating a related antibody, DATK32, that targets $\alpha_4\beta_7$, a subset of the β_7-positive integrin lymphocyte population that is targeted by FIB504.64 and found that it provides less focal uptake than FIB504.64 and that the colitis-to-control animal uptake ratio in the intestine was lower. We also evaluated 2 fragments of FIB504.64, Fab and F(ab′)$_2$, to determine whether their uptake in the target was similar to that observed for the intact antibody whereas simultaneously providing faster clearance from nontarget tissues, and found that FIB504.64-Fab is not well retained in the diseased gut. In contrast, ^{64}Cu-labeled FIB504.64-F(ab′)$_2$ has high and persistent uptake in inflamed gut combined with rapid clearance from nontarget tissues. Thus, future work will focus on ^{64}Cu-labeled FIB504.64-F(ab′)$_2$, including its comparison with other imaging biomarkers of colitis such as radiolabeled leukocytes, [^{18}F]FDG, and magnetic resonance imaging in a more clinically relevant model of colitis.

ACKNOWLEDGMENTS

The authors express their gratitude to Erin Snay and Patricia Dunning for technical assistance.

REFERENCES

1. Loftus EV Jr, Sandborn WJ. Epidemiology of inflammatory bowel disease. *Gastroenterol Clin North Am.* 2002;31:1–20.
2. Baron JH, Connell AM, Lennard-Jones JE. Variation between observers in describing mucosal appearances in proctocolitis. *Br Med J.* 1964;1: 89–92.
3. Johansson-Lindbom B, Agace WW. Generation of gut-homing T cells and their localization to the small intestinal mucosa. *Immunol Rev.* 2007;215: 226–242.
4. Shaw SK, Brenner MB. The beta 7 integrins in mucosal homing and retention. *Semin Immunol.* 1995;7:335–342.
5. Dearling JL, Park EJ, Dunning P, et al. Detection of intestinal inflammation by MicroPET imaging using a (64)Cu-labeled anti-beta(7) integrin antibody. *Inflamm Bowel Dis.* 2010;16:1458–1466.
6. Hamann A, Andrew DP, Jablonski-Westrich D, et al. Role of alpha 4-integrins in lymphocyte homing to mucosal tissues in vivo. *J Immunol.* 1994;152:3282–3293.
7. Milenic DE, Yokota T, Filpula DR, et al. Construction, binding properties, metabolism, and tumor targeting of a single-chain Fv derived from the pancarcinoma monoclonal antibody CC49. *Cancer Res.* 1991;51(23 pt 1): 6363–6371.
8. Kullmann F, Messmann H, Alt M, et al. Clinical and histopathological features of dextran sulfate sodium induced acute and chronic colitis associated with dysplasia in rats. *Int J Colorectal Dis.* 2001;16:238–246.
9. Cooper HS, Murthy SN, Shah RS, et al. Clinicopathologic study of dextran sulfate sodium experimental murine colitis. *Lab Invest.* 1993;69:238–249.
10. Okayasu I, Hatakeyama S, Yamada M, et al. A novel method in the induction of reliable experimental acute and chronic ulcerative colitis in mice. *Gastroenterology.* 1990;98:694–702.
11. Becker C, Fantini MC, Neurath MF. High resolution colonoscopy in live mice. *Nat Protoc.* 2006;1:2900–2904.
12. Vosjan MJ, Perk LR, Visser GW, et al. Conjugation and radiolabeling of monoclonal antibodies with zirconium-89 for PET imaging using the bifunctional chelate p-isothiocyanatobenzyl-desferrioxamine. *Nat Protoc.* 2010;5:739–743.
13. Maheshwari V, Dearling JLJ, Treves ST, et al. Measurement of the rate of copper(II) exchange for ^{64}Cu complexes of bifunctional chelators. *Inorg Chim Acta.* 2012;393:318–323.
14. Peer D, Park EJ, Morishita Y, et al. Systemic leukocyte-directed siRNA delivery revealing cyclin D1 as an anti-inflammatory target. *Science.* 2008;319:627–630.
15. Loening AM, Gambhir SS. AMIDE: a free software tool for multimodality medical image analysis. *Mol Imaging.* 2003;2:131–137.
16. Rivera-Nieves J, Olson T, Bamias G, et al. L-selectin, alpha 4 beta 1, and alpha 4 beta 7 integrins participate in CD4+ T cell recruitment to chronically inflamed small intestine. *J Immunol.* 2005;174:2343–2352.
17. Park EJ, Mora JR, Carman CV, et al. Aberrant activation of integrin alpha4beta7 suppresses lymphocyte migration to the gut. *J Clin Invest.* 2007;117:2526–2538.
18. Garrett WS, Lord GM, Punit S, et al. Communicable ulcerative colitis induced by T-bet deficiency in the innate immune system. *Cell.* 2007;131: 33–45.
19. Schauer DA, Linton OW. NCRP Report No. 160, Ionizing Radiation Exposure of the Population of the United States, medical exposure—are we doing less with more, and is there a role for health physicists? *Health Phys.* 2009;97:1–5.
20. Ranganathan P, Jayakumar C, Santhakumar M, et al. Netrin-1 regulates colon-kidney cross talk through suppression of IL-6 function in a mouse model of DSS-colitis. *Am J Physiol Renal Physiol.* 2013;304:F1187–F1197.
21. Ranganathan P, Jayakumar C, Manicassamy S, et al. CXCR2 knockout mice are protected against DSS-colitis-induced acute kidney injury and inflammation. *Am J Physiol Renal Physiol.* 2013;305: F1422–F1427.